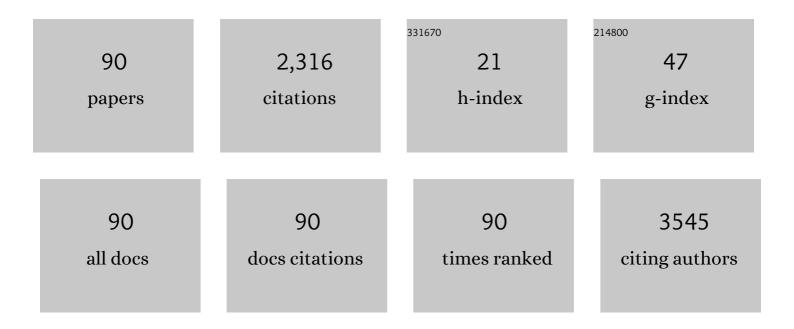
List of Publications by Year in descending order

Source: https://exaly.com/author-pdf/3935746/publications.pdf Version: 2024-02-01



WEIXING YU

#	Article	IF	CITATIONS
1	Oxygen Vacancy Enhanced Photocatalytic Activity of Pervoskite SrTiO <sub>3</sub> . ACS Applied Materials & Interfaces, 2014, 6, 19184-19190.	8.0	608
2	Microfluidic reactors for photocatalytic water purification. Lab on A Chip, 2014, 14, 1074-1082.	6.0	151
3	Metamaterialâ€Based Two Dimensional Plasmonic Subwavelength Structures Offer the Broadest Waveband Light Harvesting. Advanced Optical Materials, 2013, 1, 43-49.	7.3	150
4	A new method for the design of the heliostat field layout for solar tower power plant. Renewable Energy, 2010, 35, 1970-1975.	8.9	126
5	Plasmonic Nanolithography: A Review. Plasmonics, 2011, 6, 565-580.	3.4	90
6	Beam shaping of complex amplitude with separate constraints on the output beam. Optics Express, 2015, 23, 1052.	3.4	78
7	A new code for the design and analysis of the heliostat field layout for power tower system. Solar Energy, 2010, 84, 685-690.	6.1	66
8	Continuous artificial synthesis of glucose precursor using enzyme-immobilized microfluidic reactors. Nature Communications, 2019, 10, 4049.	12.8	60
9	Single-step fabrication of continuous surface relief micro-optical elements in hybrid sol-gel glass by laser direct writing. Optics Express, 2002, 10, 443.	3.4	57
10	Numerical study of the meta-nanopyramid array as efficient solar energy absorber. Optical Materials Express, 2013, 3, 1187.	3.0	51
11	SCECam: a spherical compound eye camera for fast location and recognition of objects at a large field of view. Optics Express, 2017, 25, 32333.	3.4	46
12	A review of available methods for surface shape measurement of solar concentrator in solar thermal power applications. Renewable and Sustainable Energy Reviews, 2012, 16, 2539-2544.	16.4	45
13	Rough gold films as broadband absorbers for plasmonic enhancement of TiO2 photocurrent over 400–800 nm. Scientific Reports, 2016, 6, 33049.	3.3	42
14	Tracking and ray tracing equations for the target-aligned heliostat for solar tower power plants. Renewable Energy, 2011, 36, 2687-2693.	8.9	39
15	A review of available methods for the alignment of mirror facets of solar concentrator in solar thermal power system. Renewable and Sustainable Energy Reviews, 2014, 32, 76-83.	16.4	31
16	Review on optofluidic microreactors for artificial photosynthesis. Beilstein Journal of Nanotechnology, 2018, 9, 30-41.	2.8	28
17	Photocatalytic reduction of Cr( <scp>vi</scp> ) by polyoxometalates/TiO <sub>2</sub> electrospun nanofiber composites. RSC Advances, 2014, 4, 44322-44326.	3.6	27
18	Plasmonic Black Absorbers for Enhanced Photocurrent of Visible‣ight Photocatalysis. Advanced Optical Materials, 2017, 5, 1600399.	7.3	26

WEIXING YU

#	Article	IF	CITATIONS
19	Ray tracing and simulation for the beam-down solar concentrator. Renewable Energy, 2013, 50, 161-167.	8.9	25
20	Germanium nanopyramid arrays showing near-100% absorption in the visible regime. Nano Research, 2015, 8, 2216-2222.	10.4	24
21	Meta-microwindmill structure with multiple absorption peaks for the detection of ketamine and amphetamine type stimulants in terahertz domain. Optical Materials Express, 2014, 4, 1876.	3.0	22
22	Dielectrophoresis-actuated in-plane optofluidic lens with tunability of focal length from negative to positive. Optics Express, 2018, 26, 6532.	3.4	22
23	Functional nanostructured surfaces in hybrid sol–gel glass in large area for antireflective and super-hydrophobic purposes. Journal of Materials Chemistry, 2012, 22, 17328.	6.7	21
24	The Talbot effect of plasmonic nanolenses. Optics Express, 2011, 19, 19365.	3.4	20
25	TiO <sub>2</sub> nanosheet array thin film for self-cleaning coating. RSC Advances, 2015, 5, 9861-9864.	3.6	20
26	Optofluidic UV-Vis spectrophotometer for online monitoring of photocatalytic reactions. Scientific Reports, 2016, 6, 28928.	3.3	20
27	Clam-inspired nanoparticle immobilization method using adhesive tape as microchip substrate. Sensors and Actuators B: Chemical, 2016, 222, 106-111.	7.8	20
28	UV induced controllable volume growth in hybrid sol-gel glass for fabrication of a refractive microlens by use of a grayscale mask. Optics Express, 2003, 11, 2253.	3.4	19
29	Multispectral curved compound eye camera. Optics Express, 2020, 28, 9216.	3.4	19
30	Biomimetic microchannels of planar reactors for optimized photocatalytic efficiency of water purification. Biomicrofluidics, 2016, 10, 014123.	2.4	18
31	Subtle control on hierarchic reflow for the simple and massive fabrication of biomimetic compound eye arrays in polymers for imaging at a large field of view. Journal of Materials Chemistry C, 2016, 4, 108-112.	5.5	17
32	Graphene on meta-surface for super-resolution optical imaging with a sub-10 nm resolution. Optics Express, 2017, 25, 14494.	3.4	17
33	Graphene–Silver Hybrid Metamaterial for Tunable and High Absorption at Mid-Infrared Waveband. IEEE Photonics Technology Letters, 2018, 30, 475-478.	2.5	17
34	A simple method for fabrication of thick sol-gel microlens as a single-mode fiber coupler. IEEE Photonics Technology Letters, 2003, 15, 1410-1412.	2.5	16
35	Fabrication of diffractive optical elements on 3-D curved surfaces by capillary force lithography. Optics Express, 2010, 18, 15009.	3.4	16
36	Fabrication and characterization of a polymeric curved compound eye. Journal of Micromechanics and Microengineering, 2019, 29, 055008.	2.6	16

#	Article	IF	CITATIONS
37	Lithographic fabrication of diffractive optical elements in hybrid sol-gel glass on 3-D curved surfaces. Optics Express, 2010, 18, 25102.	3.4	14
38	Variable surface profile gratings in sol-gel glass fabricated by holographic interference. Optics Express, 2003, 11, 1925.	3.4	13
39	Broadband efficient light absorbing in the visible regime by a metananoring array. Annalen Der Physik, 2014, 526, 112-117.	2.4	13
40	Binary amplitude-only image reconstruction through a MMF based on an AE-SNN combined deep learning model. Optics Express, 2020, 28, 30048.	3.4	13
41	Hierarchical TiO <sub>2</sub> spheres decorated with Au nanoparticles for visible light hydrogen production. RSC Advances, 2015, 5, 21237-21241.	3.6	11
42	Imaging properties of generalized composite aperiodic zone plates. Optics Express, 2020, 28, 27181.	3.4	11
43	Enhanced Photoluminescence of Monolayer MoSe <sub>2</sub> in a Double Resonant Plasmonic Nanocavity with Fano Resonance and Mode Matching. Laser and Photonics Reviews, 2022, 16, .	8.7	11
44	Patternable hybrid sol–gel material cuts the cost of fabrication of microoptical elements for photonics applications. Journal of Materials Chemistry, 2004, 14, 821-823.	6.7	10
45	Replication and characterization of the compound eye of a fruit fly for imaging purpose. Applied Physics Letters, 2014, 105, 143705.	3.3	10
46	Gradient Permittivity Meta-Structure model for Wide-field Super-resolution imaging with a sub-45 nm resolution. Scientific Reports, 2016, 6, 23460.	3.3	9
47	A compact bionic compound eye camera for imaging in a large field of view. Optics and Laser Technology, 2021, 135, 106705.	4.6	9
48	Fabrication of a Polymeric Optical Waveguide-On-Flex Using Electrostatic-Induced Lithography. IEEE Photonics Technology Letters, 2010, 22, 957-959.	2.5	8
49	Meta-nanocavity model for dynamic super-resolution fluorescent imaging based on the plasmonic structure illumination microscopy method. Optics Express, 2017, 25, 3863.	3.4	8
50	Biomimetic multispectral curved compound eye camera for real-time multispectral imaging in an ultra-large field of view. Optics Express, 2021, 29, 33346.	3.4	8
51	Investigating hybridization schemes of coupled split-ring resonators by electron impacts. Optics Express, 2015, 23, 20721.	3.4	7
52	Super-Resolution Imaging at Mid-Infrared Waveband in Graphene-nanocavity formed on meta-surface. Scientific Reports, 2016, 6, 37898.	3.3	7
53	Numerical analysis of wide-field optical imaging with a sub-20 nm resolution based on a meta-sandwich structure. Scientific Reports, 2017, 7, 1328.	3.3	7
54	Localized self-volume growth in hybrid sol-gel glass induced by ultraviolet radiation with a gray-scale mask. Applied Optics, 2004, 43, 575.	2.1	6

#	Article	IF	CITATIONS
55	Strong Intensity Modulation of Surface Plasmon Polaritons by a Dielectric Layer. IEEE Photonics Technology Letters, 2012, 24, 2214-2217.	2.5	6
56	On the Use of Silver Nanoparticles for Direct Micropatterning on Polyimide Substrates. IEEE Nanotechnology Magazine, 2012, 11, 139-147.	2.0	6
57	Reversible optical binding force in a plasmonic heterodimer under radially polarized beam illumination. Optics Express, 2020, 28, 3000.	3.4	6
58	Fabrication of multilevel structures in self-development photosensitive hybrid sol-gel glass by a gray scale mask. Optical Engineering, 2003, 42, 3411.	1.0	5
59	Hierarchic random nanosphere model for broadband solar energy absorbers. Optical Materials Express, 2015, 5, 2777.	3.0	5
60	Photocatalytic ozonation for sea water decontamination. Journal of Water Process Engineering, 2020, 37, 101501.	5.6	5
61	Volume growth initiated by point-to-point ultraviolet-laser direct writing in hybrid solgel glass for three-dimensional microfabrication. Optics Letters, 2003, 28, 1573.	3.3	4
62	Negative Refraction and Focusing of Photonic Crystals with Graded Negative Index in Visible Regime. Plasmonics, 2013, 8, 335-340.	3.4	4
63	Fabrication of refractive silicon microlens array with a large focal number and accurate lens profile. Microsystem Technologies, 2020, 26, 1159-1166.	2.0	4
64	Tailorable polygon-like beams generated by modified spiral petal-like zone plates. Results in Physics, 2021, 21, 103823.	4.1	4
65	Computational Study of Influence of Structuring of Plasmonic Nanolens on Superfocusing. Plasmonics, 2011, 6, 35-42.	3.4	3
66	Study of the Plasmon Talbot Effect of Metallic Nanolenses Induced by Linearly Polarized Illumination. Plasmonics, 2012, 7, 641-645.	3.4	3
67	Planar polarization-routing optical cross-connects using nematic liquid crystal waveguides. Optics Express, 2018, 26, 402.	3.4	3
68	Colourful imaging and self-reconstruction properties of modified single-focus fractal zone plates. Optics Express, 2020, 28, 37827.	3.4	3
69	Three tailorable optical vortices generated by a modified fractal spiral forked plate. Journal of Optics (United Kingdom), 2021, 23, 045603.	2.2	2
70	Multiple-Beam Surface Plasmon Holographic Nanolithography. Plasmonics, 2013, 8, 561-569.	3.4	1
71	Investigation of Focusing Characteristics of Plasmonic Lenses with Concentric Elliptical Slits. Journal of Computational and Theoretical Nanoscience, 2013, 10, 2609-2617.	0.4	1
72	A Method for the Micro-encapsulation of Dielectric Fluids in Joined Polymer Shells. Current Organic Chemistry, 2013, 17, 65-71.	1.6	1

#	Article	IF	CITATIONS
73	Si Substrate-Based Metamaterials for Ultrabroadband Perfect Absorption in Visible Regime. Journal of Nanomaterials, 2014, 2014, 1-5.	2.7	1
74	Influence of electrode types on the electrohydrodynamic instability patterning process: a comparative study. RSC Advances, 2016, 6, 112300-112306.	3.6	1
75	Polarization and sizes variation immune optical absorbers. Modern Physics Letters B, 2016, 30, 1650010.	1.9	1
76	Numerical study of the faithful replication of micro/nanostructures on curved surfaces by the electrohydrodynamic instability process. Electrophoresis, 2017, 38, 525-532.	2.4	1
77	Fabrication and experimental characterization of precise high-efficiency 2D multi-mode fiber array coupler. Optical Fiber Technology, 2021, 63, 102488.	2.7	1
78	Characterization of TiO/sub 2//SiO/sub 2/ hybrid sol-gel glass and its use for fabrication of micro-optical elements. , 0, , .		0
79	Immersed nanospheres super-lithography for the fabrication of sub-70nm nanoholes with period below 700nm. , 2012, , .		0
80	A composite hardness stamp in 184 PDMS for nanostructures transfer in high fidelity. , 2012, , .		0
81	Formulation of the finite-difference time-domain method for the analysis of axially symmetric metal nanodevices. Journal of Modern Optics, 2012, 59, 1439-1447.	1.3	Ο
82	Study of Metallic Nanowires with Arbitrary Cross-Sectional Shapes for Negative Refraction in Visible Regime. Plasmonics, 2012, 7, 619-626.	3.4	0
83	Nano-multiwall cylinders array for ultra-broadband perfect absorption in visible regime: novel properties revealing. Modern Physics Letters B, 2014, 28, 1450086.	1.9	0
84	Electron impact investigation of hybridization scheme in coupled split-ring resonators. , 2014, , .		0
85	Investigation of enhancement of near-field probing for sensing at terahertz waveband. Optik, 2015, 126, 4823-4826.	2.9	0
86	Noise analysis of the Vernier anode. Applied Optics, 2015, 54, 6904.	2.1	0
87	Photocatalysis: Plasmonic Black Absorbers for Enhanced Photocurrent of Visible‣ight Photocatalysis (Advanced Optical Materials 2/2017). Advanced Optical Materials, 2017, 5, .	7.3	0
88	Fabrication of hollow polymer microstructures using dielectric and capillary forces. Microsystem Technologies, 2020, 26, 301-308.	2.0	0
89	A Polygon-Like Light-Arm Zone Plate. IEEE Photonics Technology Letters, 2022, 34, 355-358.	2.5	0
90	Extended bifocal depth imaging with modified generalized composite kinoform Fibonacci lenses. Optics and Laser Technology, 2022, 152, 108162.	4.6	0